A fragment of Argoland from East Gondwana in the NE Himalaya

Ji'en Zhang[1], Wenjiao Xiao[1, 2], John Wakabayashi[3], Brian F. Windley[4], Chunming Han[1]

[1] State Key Laboratory of Lithospheric Evolution, Institute of Geology and Geophysics, Chinese Academy of Sciences, Beijing 100029 China.

[2] Xinjiang Research Center for Mineral Resources, Xinjiang Institute of Ecology and Geography, Chinese Academy of Sciences, Urumqi 830011 China.

[3] Department of Earth and Environmental Sciences, California State University, Fresno, CA 93740 USA.

[4] School of Geography, Geology and the Environment, University of Leicester, Leicester LE1 7RH, UK.

Corresponding author: Ji'en Zhang (zhangjien@mail.iggcas.ac.cn)

Key Points:

- The Longzi block in the NE Himalaya records Early Cretaceous shortening and Late Jurassic alkali magmatism
- First geological evidence presents the Longzi block as a westernmost fragment of Argoland from East Gondwana
- Archipelagic framework since Late Jurassic impacts Mesozoic geodynamics of Neotethyan and Cenozoic collisional processes in East Asia

Abstract

Previous studies have concluded that a Trans-Tethyan oceanic subduction zone existed prior collision of India-Eurasian plates, between which the ocean lacked intervening continental slivers. In contrast, we present first geological evidence of Early Cretaceous shortening and Late Jurassic alkali magmatism constraining that the Longzi block, an extensive (>450 km E-W by ca. 130 km N-S) tract of the NE Himalaya is such a continental sliver. The Longzi block records overturned south-vergent folds in Triassic to Lower Cretaceous strata intruded by 136-123 Ma mafic, dioritic, and dacite dikes, constraining Early Cretaceous shortening. The shortening demonstrates the NE Himalayan locating in a compressional setting, rather than an extensional Indian passive continental margin at that time. Triassic strata of NW Australian affinity and Late Jurassic rocks sourced from north India record pre-rifting history. Rifting evidence includes 152.8 Ma alkali intrusive rocks, a Late Jurassic unconformity, and rapid changes in sediment thickness and apparent water depth of deposition recorded in Upper Jurassic strata. The rifting event is coeval with 152-155 Ma oceanic crust in the NE Indian Ocean and a Late Jurassic submarine escarpment with 1200 m of sediments offshore of NW Australia. These data may reflect rifting of the westernmost Argoland continent in NE Himalaya from East Gondwana, followed by collision with a N-dipping Trans-Tethyan intra-oceanic subduction zone in the Early Cretaceous, long before terminal continent-continent collision. The Mesozoic rifting-collision in the Himalayan region unambiguously presents archipelagic paleogeography in eastern Neotethyan, which underwent Cenozoic two-stage Indian-Eurasian collisional processes.

1 Introduction

Paleogeography in the Himalayan region, southern Tibet, is crucial to reconstruct Mesozoic geodynamics of Neotethyan regime in East Asia, and collisional processes between the East Gondwana and Eurasian plates (Fig. 1a) (Jagoutz et al., 2015; van Hinsbergen et al., 2012, 2019; Yin & Harrison, 2000; Yuan et al., 2020). Three end-member models have been proposed to explain the geologic affinity of the Himalaya as: (1) a continental block separated from Indian plate at 118 Ma (van Hinsbergen et al., 2012, 2019), (2) the northern continental margin of Indian craton (Yin & Harrison, 2000; Zhu et al., 2007), or (3) an accretionary complex created by Neo-Tethys Ocean subduction between 130 Ma and 50 Ma (Ao et al., 2018). The former two models supposed that the Tethyan Himalaya attached to East Gondwana at ca. 130 Ma (Fig. 1c). At this time the Gondwana and Eurasian plates were separated ~8000 km by the Neo-Tethys Ocean (Jagoutz et al., 2015; van Hinsbergen et al., 2019) that was generally assumed to be an entirely oceanic realm, including SSZ-type ophiolites and a Trans-Tethyan intra-oceanic subduction system (including the Zedang arc) (Aitchison et al., 2000; Hébert et al., 2012; McDermid et al., 2002).

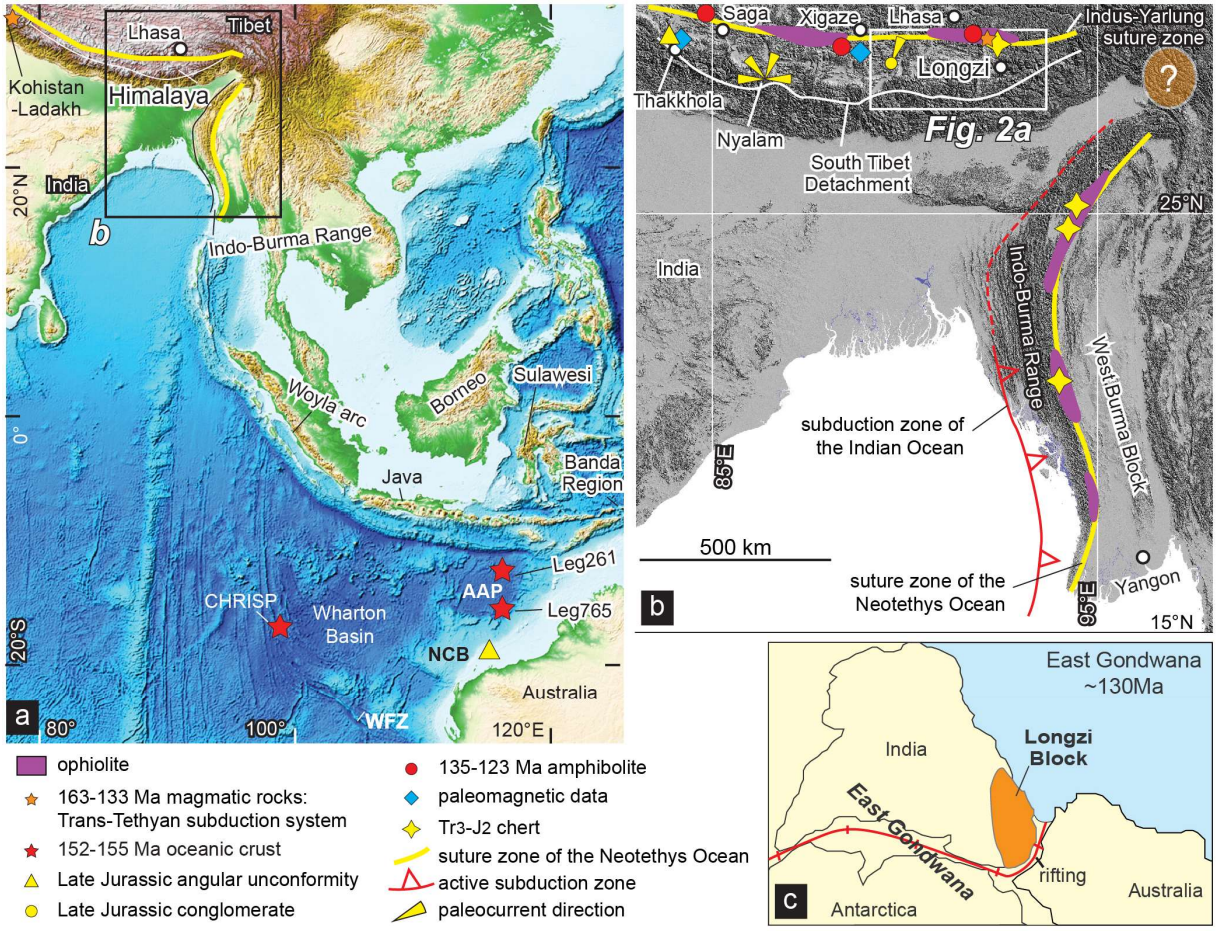

Figure 1. (**a**) Schematic map of southern Tibet, SE Asia, NW Australia and NE Indian Ocean, showing tectonic units and locations of Late Jurassic oceanic crust. The Argoland-derived fragments in SE Asia, such as Indo-Burma Range, West Sulawesi, SW Borneo, East Java and Woyla arc are presented (Advokaat et al., 2018; Metcalf, 2011; Zahirovic et al., 2016). Base map is from National Oceanic and Atmospheric Administration (2012). (**b**) Tectonic units developed in south Tibet and the Indo-Myanmar belt, showing the location of NE Himalaya in Fig. 2a. Paleomagnetic data in Cretaceous is from Yuan et al. (2020) and in Triassic is from Klootwijk and Bingham (1980). Locations of amphibolites of metamorphic soles are from Guilmette et al. (2009, 2012) and Zhang et al. (2016a). Ages of chert in ophiolitic mélange and interlayered siltstone and chert are from Aitchison et al. (2019), Chen et al., (2019), and Zhang et al. (2018). Paleocurrent directions determined by cross beddings of Late Jurassic and Triassic sediments are from Li et al. (2003), Pan (2018) and Zhang et al. (2019). Late Jurassic angular unconformity in NW Australia is from Gradstern (1992), and in south Tibet is from Garzanti (1999). (**c**) Generalized plate tectonic reconstruction in East Gondwana in ca. 130 Ma, showing the Longzi block attached northeastern Indian plate and western Australian plate (Harry et al., 2020; Zhu et al., 2007). Acronyms: AAP: Argo Abyssal Plain, NCB: North Carnarvon Basin, WFZ: Wallaby fracture zone.

In SE Asia, continental fragments from the Wallaby fracture zone to the Banda region, and Indo-Burma Range, known as the Argoland sliver, had been rifted off of the NW Australia margin (Gibbons et al., 2012, 2015; Hall, 2012; Metcalfe, 2011; Veevers et al., 1991; Zahirovic et al., 2016), beginning at 152-155 Ma based on isotopic and fossil ages and magnetic anomaly from the NE Indian Ocean (Fig. 1a) (Gibbons et al., 2012; Heine & Muller, 2005; Zahirovic et al., 2016). This sliver drifted northwards prior to Early Cretaceous India-Australia separation (Harry et al., 2020).

Triassic sediments in the NE Himalaya share Late Triassic Halobia sp., and detrital zircons of 1250-900 and 750-450 Ma, and 400-200 Ma-aged magmatic zircons with $\varepsilon_{Hf}(t)$ values of -10 - +14 (Cai et al., 2016; Liu et al., 2020; Wang et al., 2016a) with those from the Indo-Burma Range (Yao et al., 2017), suggesting that they approached each other (Fig. 1b). The Late Jurassic separation of the Indo-Burma Range from the NW Australia (Gibbons et al., 2012, 2015; Metcalfe, 2011; Zahirovic et al., 2016) hints that NE Himalaya should have a similar tectonic history.

Paleomagnetic data suggest that the Tethyan Himalaya was still at the same latitude as Gondwana in the Early Cretaceous (van Hinsbergen et al., 2019 and references therein), but it cannot negate the possibility of longitudinal separation. To identify such a separation of the NE Himalaya from Gondwana, three diagnostic features are required: (i) Prior to the Late Jurassic, the NE Himalaya was attached to East Gondwana; and it underwent (ii) Late Jurassic extension and (iii) post-rifting and contractional deformation, which was not recorded in the Indian plate, and predated terminal (India-Eurasia) collision.

In the Tethyan Himalaya, ages of deformation in unmetamorphosed strata are generally difficult to constrain because of lack of syn-deformational mineral growth (Searle & Treloar, 2019). In the NE Himalaya, however, Early Cretaceous dikes intrude asymmetric folds (Fig. 2a) helping constrain the age of early-stage deformation. In this paper we report two important findings in the NE Himalaya: (1) Early Cretaceous contractional deformation, and (2) Late Jurassic intrusive alkali mafic-ultramafic rocks, that fulfill diagnostic features (ii) and (iii). Published data demonstrate the feature (i), so we suggest that a westernmost Argoland fragment termed the “Longzi block” docked in the NE Himalaya.

2 Geological Setting

The Himalaya in south Tibet is characterized by N-dipping tectonic stacks, such as the Tethyan and the Greater Himalaya (Yin & Harrison, 2000). The Tethyan Himalaya consists of Paleozoic-Mesozoic clastics, volcanics and carbonates, covered by Paleocene-Eocene flysch (BYGS, 2004; Garzanti, 1999). It is bounded to the north by the Indus-Yarlung suture zone, the Neo-Tethys Ocean suture zone (Hébert et al., 2012) connecting with eastern margin of the Indo-Burma Range (Fig. 1b) (Zhang et al., 2018). To the south, the South Tibet Detachment separates the Tethyan Himalaya from the crystalline Greater Himalaya.

The >450 km E-W by ca. 130 km N-S Longzi region in the NE Tethyan Himalaya (Fig. 1b), that we term the Longzi block, exposes Late Triassic-Middle Jurassic turbidites, overlain by Late Jurassic conglomerates (such as the Weimei Formation), Early Cretaceous to Late Cretaceous turbidites, and Eocene olistostromes in the north, and Paleozoic strata that are unconformably overlain by Late Triassic coastal eolian dune deposits and Early Cretaceous sediments in the south (Fig. 2a) (BYGS, 2004; Pan, 2018). Some Mid-Late Triassic and Early

Cretaceous dikes have negative $\varepsilon_{Nd}(t)$ (-13.4 - -0.1) and $\varepsilon_{Hf}(t)$ (-24.2 - -0.1) (Huang et al., 2018; Liu et al., 2020; Wang et al., 2016b; Zhu et al., 2007).

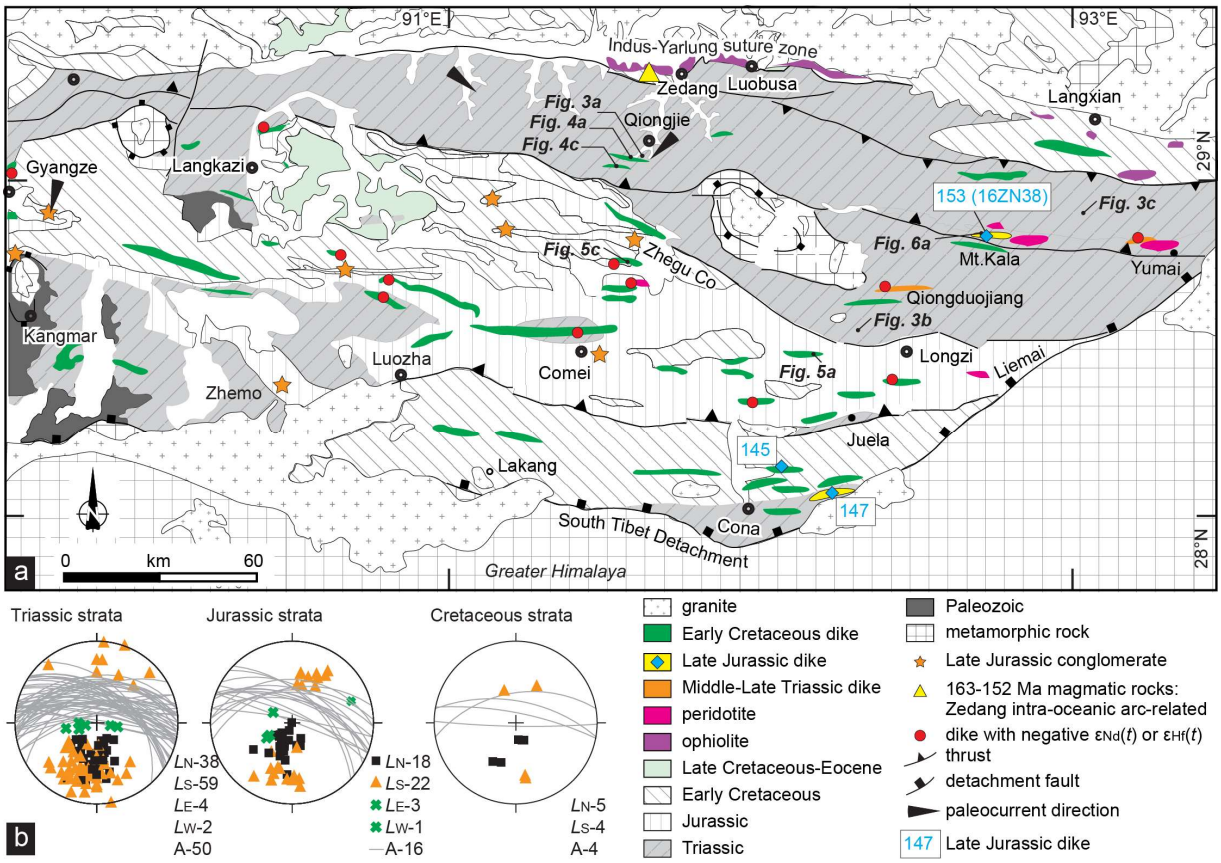

Figure 2. (**a**) Geological map of the NE Himalaya (BYGS, 2004). The locations of Late Jurassic dikes, dikes with negative $\varepsilon_{Nd}(t)$ and $\varepsilon_{Hf}(t)$, and Late Jurassic conglomerate are marked. The paleocurrent directions determined by cross bedding of Late Jurassic quartz sandstone and Triassic turbidite are from Li et al. (2003), Pan (2018) and Zhang et al. (2019). The 145-147 Ma dikes are from Shi et al. (2018) and Zhu et al. (2008). (**b**) Poles to the north (L_N) and south (L_S) limbs, east (L_E) and west (L_W)-plunge beddings in an anticlinal view and axial surfaces (A) in Triassic, Jurassic and Early Cretaceous strata. The north limbs are normal; some south limbs are normal and others are overturned. Axial surfaces show that these folds strike E-W and have south-vergence.

Late Triassic sediments yield detrital zircons with 1250-900 and 750-450 Ma, and 400-200 Ma magmatic ages with $\varepsilon_{Hf}(t)$ values of -10 - +14 (Cai et al., 2016; Liu et al., 2020; Wang et al., 2016a). These zircons correlate with those from the North Carnarvon Basin, NW Australia (Lewis & Sircombe, 2013). Late Jurassic conglomerates with ENE-directed paleocurrents contain 95% quartzite pebbles, with 550 and 950 Ma detrital zircon peaks, matching the East Indian cratonic basin (Pan, 2018). The Late Jurassic stratigraphy features rapid lateral thickness changes from a few tens to a hundred meters in a continental shelf-slope setting that apparently reflects syn-depositional extension (Garzanti, 1999; Yin & Wan, 1996). The Early Cretaceous

Jiabula and Lakang Formations contain Valanginian-Albian *Olcostephanus* cf. *schenki*, *O. madagascriensis*, and *Proleymerella* sp. (BYGS, 2004).

Abundant intrusions and volcanic rocks occur in the NE Himalaya region, including an OIB-affinity trachyandensitic dike and a MORB-affinity diabase in Cona County with zircon U-Pb ages at 147 ± 2 Ma and 145 ± 2 Ma, respectively (Shi et al., 2018; Zhu et al., 2008), and gabbroic intrusions, diabase/diorite dikes, basalt, andesite, dacite and rhyolite yielding zircon U-Pb and Ar-Ar ages of 135.5-118 Ma (Fig. 2a) (Ao et al., 2018; Wang et al., 2016b; Zhu et al., 2008, 2013). Some Early Cretaceous mafic rocks have alkali affinity (Zhu et al., 2013), and some have SSZ (supra-subduction zone) affinity (Wang et al., 2016b), similar to the andesite and silicic intrusions (Ao et al., 2018). Three mafic-ultramafic rock bodies have been regarded as ophiolites in south Tibet (Fig. 2a) (Ao et al., 2018; Liu et al., 2020). However, we show they intrude sedimentary strata rather than tectonically-emplaced.

3 Results

3.1 Structural Geology

3.1.1 Folding

Triassic, Jurassic and Lower Cretaceous strata of the Longzi block exhibit well-developed flexural-slip folds, over a region more than 100 km in width from Qiongjie County (South of Zedang city) in the north to Cona County in the south (Fig. 2a). High-relief areas, such as the northern NE Himalaya, where strata comprise primarily Triassic and Jurassic rocks, feature widespread isoclinal folds (Fig. 3a), overturned folds (Figs. 3b, 4, 5a-b) and superimposed folds, which have been stacked by south-vergent thrusts. These folds have amplitudes of tens to hundreds of meters (Figs. 3a-b, 4, 5a-b). Beds generally maintain thickness, although beds in some limbs are locally boudinaged (Fig. 3c), and some beds are slightly thickened in hinge zone (Fig. 3d), suggesting these folds are parallel to Class-1c folds. Some hinge zones display axial-surface cleavages (Fig. 3d).

Figure 3. Photos showing structures related to folding in NE Himalaya. (**a**) Isoclinal folds with south-vergence to south of Qiongjie County. Note the houses at the foot of the mountains as scale. (**b**) South-vergent overturned anticline and syncline to west of the Longzi County strike to E-W and their limbs preserve boudinages (**c**). (**d**) Overturned anticline to south of Qiongjie County has overturned south limb and develops axial-surface cleavages dipping north. Its location is marked in Fig. 4c.

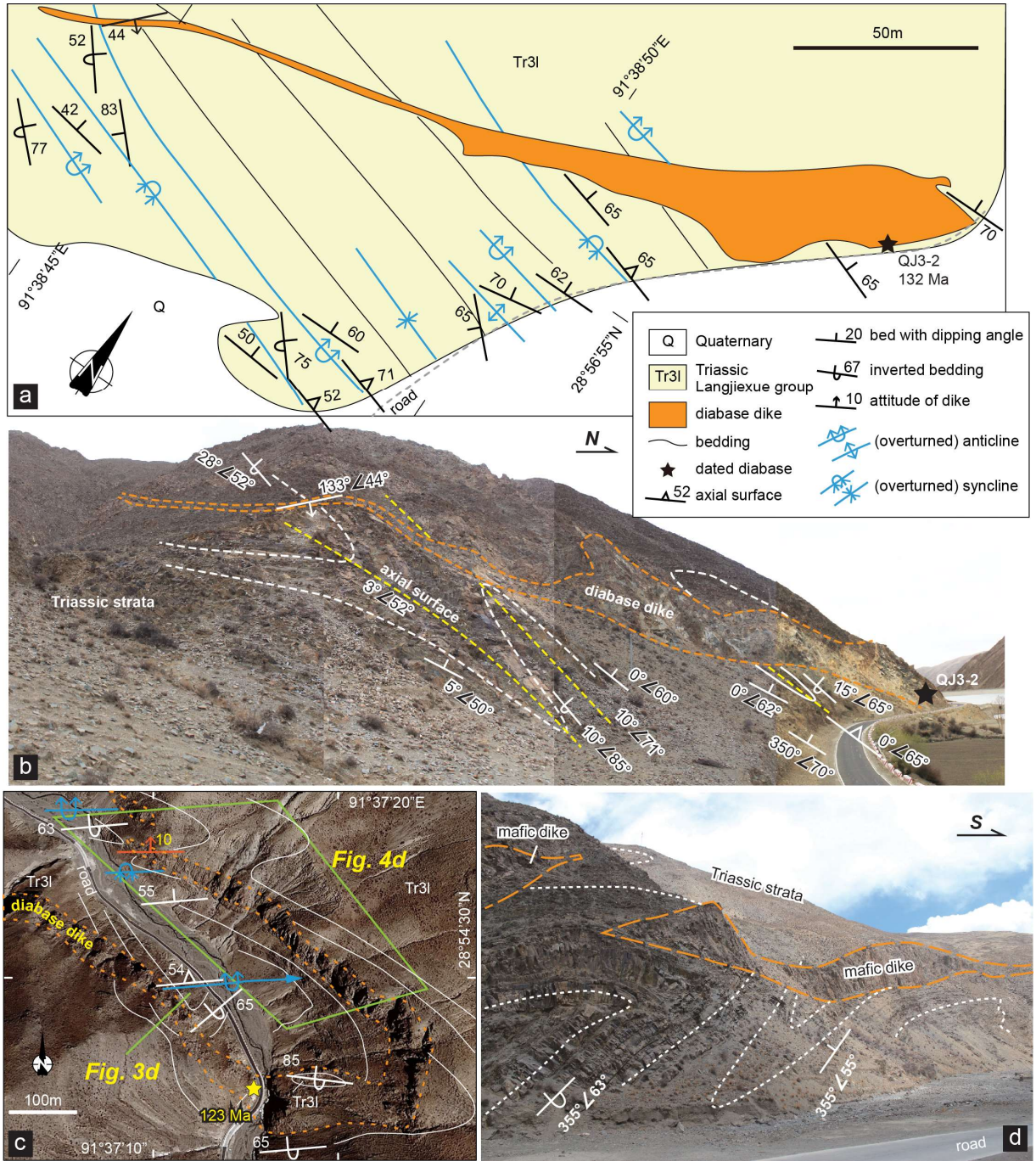

Figure 4. Relationships between folds in Triassic strata and dikes to south of Qiongjie County. (**a**) Structural map and (**b**) photo show a NE-striking 132 Ma diabase dike obliquely cross-cutting the hinges of overturned syncline and anticline, which strike E-W. The age of the diabase dike is from Zhu et al. (2013). (**c**) Structural map and photo (**d**) show a gently north-dipping 123 Ma diabase dike cross-cutting limbs of an overturned anticline and syncline, which have south-vergence. The dike age is from BYGS (2004).

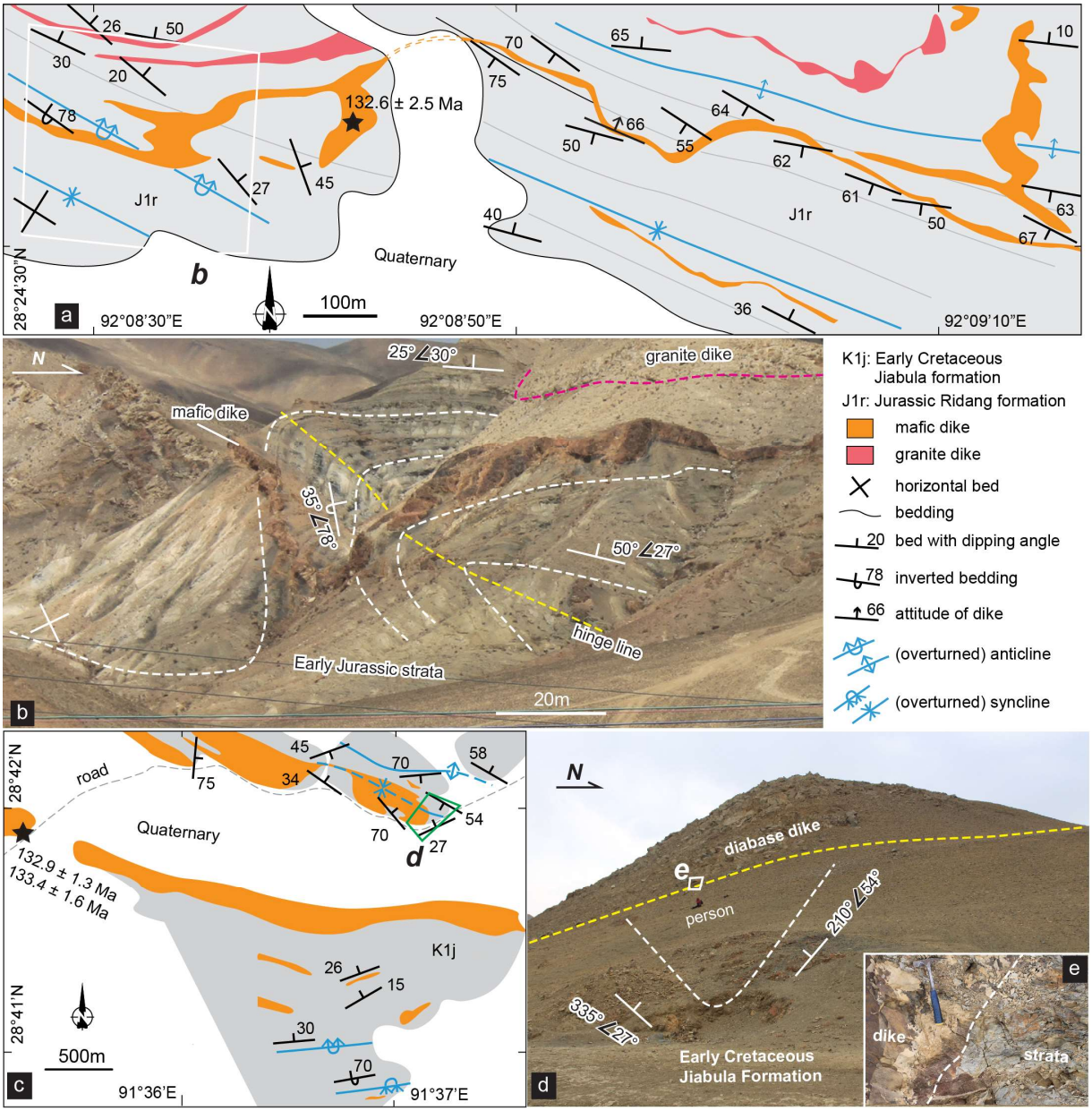

Figure 5. Relationships between folds in Jurassic and Cretaceous strata and dikes in the NE Himalaya. (**a**) Structural map and (**b**) photo show the E-W trending 133 Ma mafic dike obliquely cut the hinge of overturned anticline in Jurassic strata to west of Longzi County. The age of mafic dike is from Ao et al. (2018). (**c**) Structural map and (**d**) photo showing 133 Ma mafic dikes cross-cutting an open fold in Early Cretaceous Jiabula Formation near Zhegu Co, to south of Qiongjie County. (**e**) Photo shows the intrusive contact between Early Cretaceous strata and a mafic dike. The ages of the mafic dikes are from Zhu et al. (2013). The relations demonstrate that the folds predate the intrusion of dikes in the NE Himalaya.

In this paper, we define anticlinal fold limbs as north (L_N) and south limbs (L_S), or east and west limbs as L_E and L_W, respectively (Fig. 2b). The axial surfaces (A) are parallel with the axial-surface cleavages, or their orientation is estimated from the intersection of north and south limbs employing the β-diagram method.

Folds in Triassic strata have upright north limbs striking 45-141°, and dipping northward 26-75°; upright south limbs strike 50-137° and dip southward 65-90°. Overturned south limbs strike 50-145° and dip 32-90° northward (Fig. 2b). Axial surfaces of all folds strike 60-138° with most 80-110° and dip northward 30-90° (Fig. 2b).

North limbs of folds in Jurassic strata strike 90-145° and dip 0-75° northward; upright south limbs strike 90-126° and dip 50-75° southward, and overturned south limbs strike 100-125° and dip 48-82° northward (Fig. 2b). Axial surfaces of these folds strike 98-134° with most 100-112° and dip 43-90° northward (Fig. 2b).

Bedding in Early Cretaceous strata near Cona County has been transposed by north and south-dipping cleavage. In Zhegu Co some open and overturned folds have hundred-meter amplitudes (Fig. 5c). The open folds have upright north and south limbs striking 65-110° and 70-120°, respectively, and dipping northwards and southwards 27-55° and 45-55°, respectively (Fig. 2b). Their axial surfaces strike to 91-101° and with north to south dips of 76-85° (Fig. 2b). The overturned folds have upright north limbs striking 70-120° and dipping 24-58° northward; overturned south limbs strike 80° and dip 67-70° northward (Fig. 2b). The axial surfaces strike 80-100° and dip 50-60° northward (Fig. 2b).

In summary, asymmetric folds in the NE Himalaya show south vergence with overturned south limbs and north-dipping axial planes, and E-W-trending axes (Fig. 2b).

3.1.2 Field relationships between folds and Early Cretaceous dikes

In the NE Himalaya, abundant gabbroic intrusions, diabase/diorite dikes, basalt, andesite, dacite and rhyolite yield zircon U-Pb and ^{39}Ar-^{40}Ar ages of 135.5-118 Ma and crop out in the area from Gyangze-Kangmar in west to Longzi county in east, and from Qiongjie county in north to Cona county in south (Fig. 2a) (Ao et al., 2018; Wang et al., 2016b; Zhu et al., 2008, 2013). Most mafic rocks have alkali affinity (Zhu et al., 2013), and a few mafic, andesitic and silicic intrusions have SSZ-affinity (Ao et al., 2018; Wang et al., 2016b).

In Triassic strata south of Qiongjie County, E-W trending hinges of the overturned folds have been obliquely cross-cut by a 132 Ma mafic dike (Zhu et al., 2013), which strikes 43° (Fig. 4a-b); both limbs of asymmetric folds were intruded by a shallowly-dipping (10°) and E-W striking 123 Ma diorite dike (BYGS, 2004), which is oriented parallel to fold hinges (Fig. 4c-d).

In Jurassic strata west of Longzi County, WNW-ESE to E-W trending hinges and both limbs of asymmetric folds were obliquely cross-cut at low angle by a 133 Ma mafic dike (Ao et al., 2018), which strikes E-W and dips 66° north (Fig. 5a-b). In Cretaceous strata near Zhegu Co, both limbs of an open syncline have been cut by a shallowly-dipping 133 Ma diabase dike (Fig. 5c-d) (Zhu et al., 2013).

Above relationships show that Early Cretaceous mafic-felsic dikes intrude the folds, demonstrating that the shortening recorded by these folds predates intrusion.

3.2 Late Jurassic alkali mafic-ultramafic rocks

More than 50 km south of the Indus-Yarlung suture, several-hundred-meter by ten-meter ultramafic-mafic rock bodies crop out within Triassic and Jurassic units in the Mt. Kala, Yumai and Liemai areas (Fig. 2a, 6a) (BYGS, 2004). They include serpentinized pyroxenite, gabbro, diabase, and basaltic rocks. Most outcrops are in fault contact with host sediments. However, some massive gabbro and diabase grade into pillow basalt that is interbedded with sedimentary strata (Fig. 6b) or into basaltic dike-like intrusions a few centimeters (Liu et al., 2020) to several meters thick and tens of meters long that cut sedimentary bedding (Fig. 6b-c). Mafic rocks at Mt. Kala locally preserve original intrusive contacts with Triassic sandstone and siltstone (Fig. 6d).

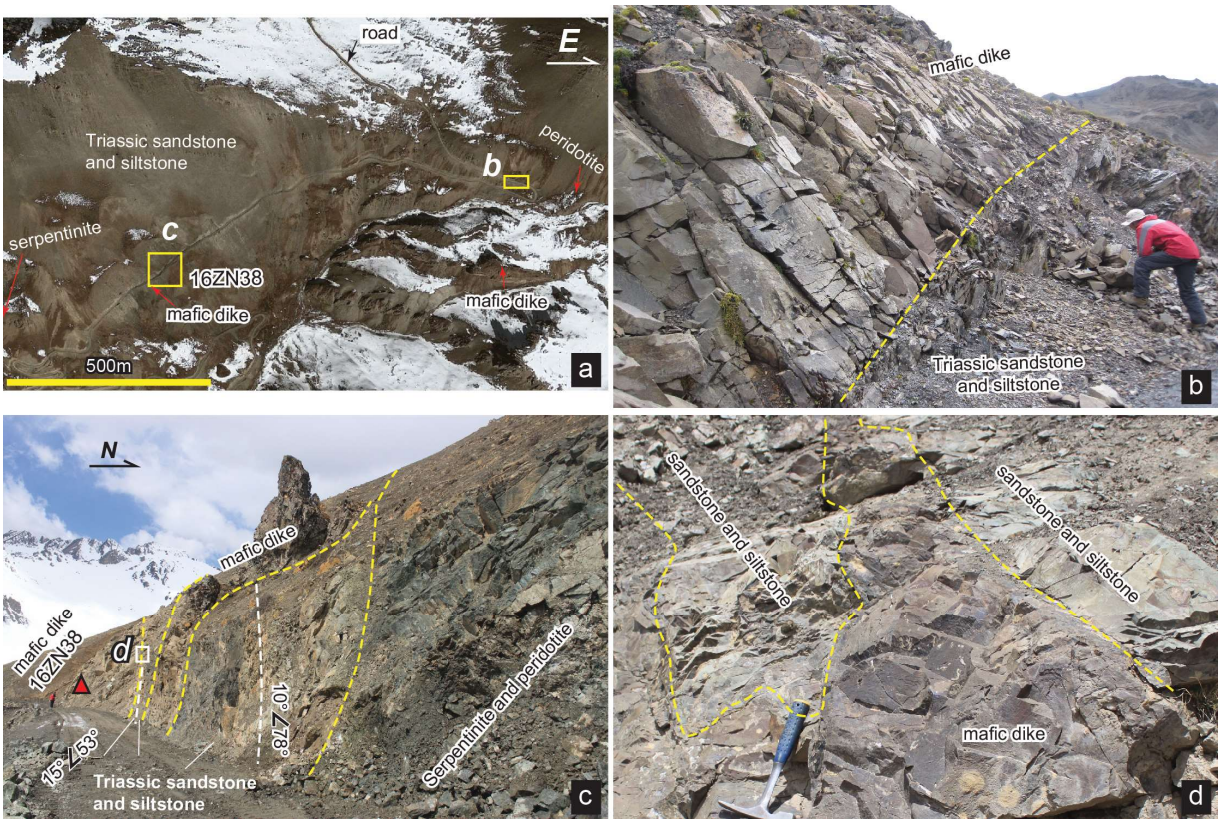

Figure 6. Relationships between Late Jurassic mafic-ultramafic rocks and Triassic turbidite in Mt. Kala. The location is marked in Fig. 2a. (**a**) Satellite image of Mt. Kala shows the locations of serpentinite, peridotite, mafic dike and Triassic sandstone and siltstone. The white cover is snow, and satellite image is from Google maps. (**b**) Thick mafic dike intruding the Triassic sandstone and siltstone. (**c**) Relationships between serpentinite, peridotite, mafic rocks and Triassic strata. The ultramafic rocks underwent alteration, and local outcrops preserve the intrusive contact between the mafic dikes and the bedding (**d**). Photo showing location of dated mafic dike sample 16ZN38.

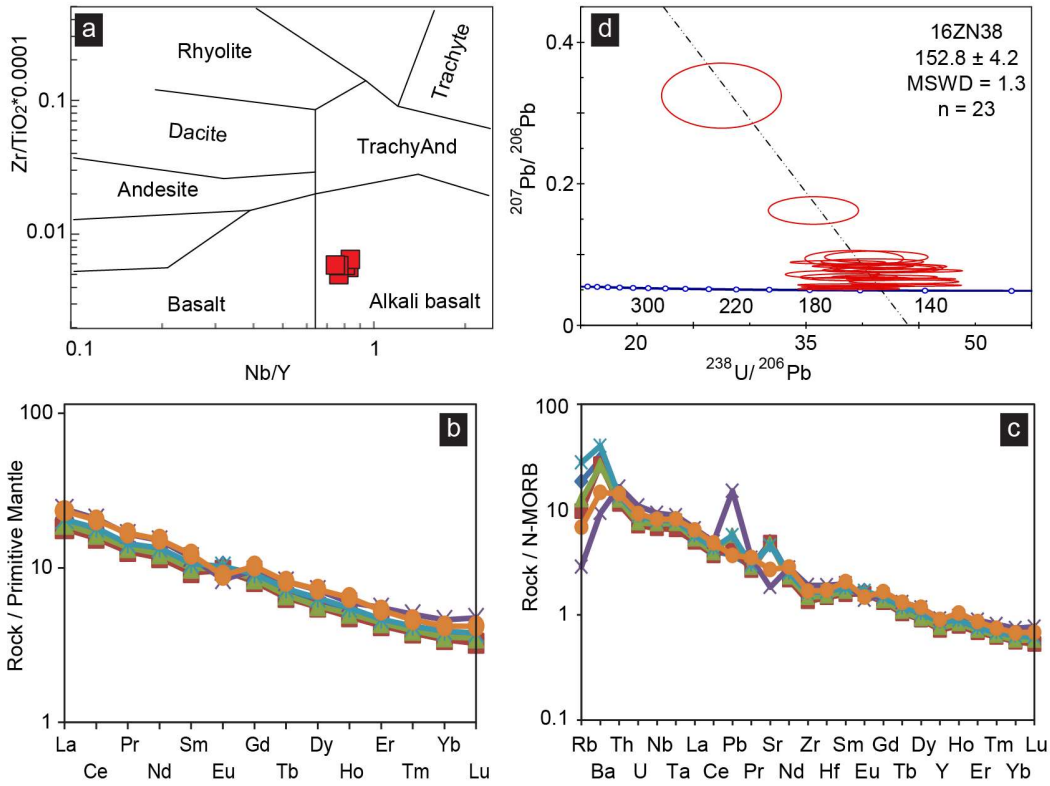

Figure 7. (**a**) Nb/Y-Zr/TiO2×0.0001 diagram of the mafic rocks from Mt. Kala (Winchester & Floyd, 1977). (**b**) Primitive mantle-normalized REE patterns and (**c**) N-MORB-normalized spider diagrams of incompatible elements of mafic rocks in Mt. Kala. Primitive mantle and N-MORB values from Sun & McDonough (1989). (**d**) SIMS baddeleyite U-Pb age of gabbro from Mt. Kala mafic-ultramafic rock body.

The mafic rocks have consistent content of SiO_2 (45.44-49.62 wt%), TiO_2 (1.85-2.18 wt%), Al_2O_3 (14.57-15.36 wt%) and MgO (5.30-6.84 wt%) (Table S2). They plot in the alkali basalt field on the Nb/Y-Zr/TiO_2 diagram (Fig. 7a). Primitive mantle-normalized diagram of trace elements shows they are enriched in LREEs (Fig. 7b) and N-MORB normalized spider diagram of incompatible elements presents that there have no anomalies of high-field strength elements (such as Nb, Ta) (Fig. 7c). These data suggest that the mafic rocks were products of alkali magmatism.

Zircons from a massive basaltic dike in the Yumai area share similar age populations as those of host Triassic sediments indicative of inherited zircons (Liu et al., 2020). Baddeleyite, in contrast, more likely crystallized in the magma chamber of the mafic rocks. Baddeleyites from a gabbro (sample 16ZN38) at Mt. Kala (Figs. 6a, c) are euhedral with sizes of 40-60 μm (Fig. S3). They yielded a U-Pb age of 152.8 ± 4.2 Ma (MSWD = 1.3, total 23 grains) (Fig. 7d) dated by Cameca SIMS-1280 at IGGCAS in Beijing (China).

4 Discussion

4.1 Early Cretaceous contractional deformation

Hinges of folds in Triassic, Jurassic and Early Cretaceous strata in the NE Himalaya trend E-W (Fig 2b), indicating N-S shortening. The hinge and limbs of these folds have been cut by 135-118 Ma dikes of gabbro, basaltic and andesitic, dacite and rhyolite (Figs. 3-5) (Chen et al., 2018; Wang et al., 2016b; Zhu et al., 2008, 2013), demonstrating that shortening in Longzi area predates these dikes. The folds involving youngest strata are the Valanginian-Albian Jiabula and Lakang Formations, which contain Valanginian-Albian *Olcostephanus* cf. *schenki*, *O. madagascriensis*, and *Proleymerella* sp. (Fig. 2a) (BYGS, 2004). These data show that the Longzi block in NE Himalaya underwent contractional deformation during the Early Cretaceous.

Some researchers indirectly assumed a ~130 Ma break-up of the northern margin of Indian plate, which contains the Longzi block, based on occurrence of OIB-affinity mafic rocks (Fig. 1c) (Zhu et al., 2013). However, such a scenario should have generated ca. 130 Ma extensional structures, in contrast with the shortening of that age recorded in the Longzi block.

The Early Cretaceous shortening of Longzi block shows that it was not part of a passive continental margin of East Gondwana that time (Fig. 8). This suggests that the Longzi block had drifted away from East Gondwana continent before the Early Cretaceous (Figs. 8, 9c). The contractional deformation, consistent with diagnostic feature iii in the Introduction section (Table 1), is not recorded in the northern margin of Indian plate and took place long before the terminal Cenozoic collision between the Indian-Asian plates (Aitchison et al., 2000; Gibbons et al., 2015; van Hinsbergen et al., 2012; Yin & Harrison, 2000).

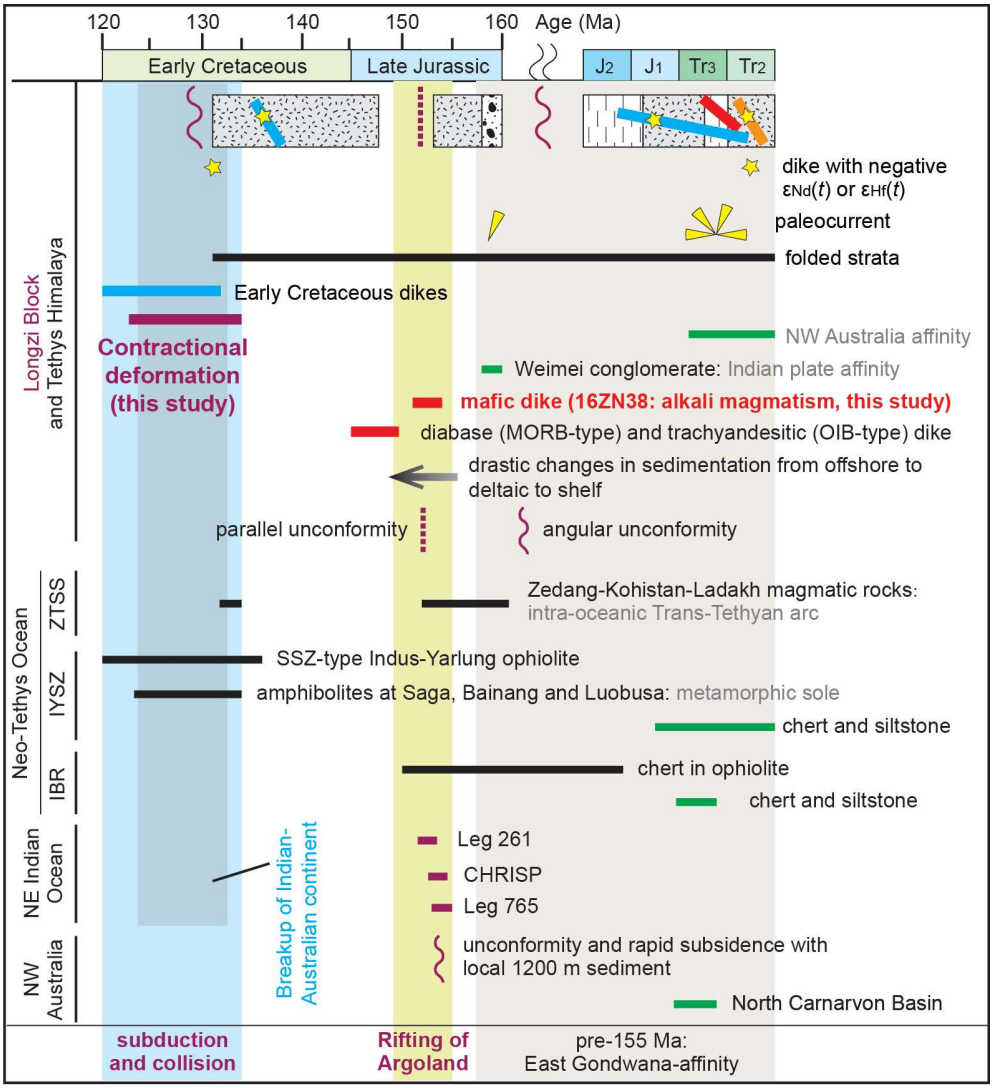

Figure 8. Time-stratigraphic relationships between dikes, folds, and sedimentary structures in Longzi block and Tethyan Himalaya and ophiolites, metamorphic sole amphibolites and ages of oceanic basins in the Neo-Tethys Ocean, NE Indian Ocean and NW Australia. They present three stages as Early Cretaceous contractional deformation in the Longzi block, which may be related to subduction and collision with Zedang/Trans-Tethyan subduction system, Late Jurassic rifting of Argoland, and pre-155 Ma East Gondwana-affinity related sedimentation and structures. See Text S1 for references. The stratigraphic column of the Longzi block is based on BYGS (2004).

Table 1. Comparison between three theoretical diagnostic features for a Late Mesozoic separated block and facts in NE Himalaya, NE Indian Ocean and NW Australia

	Evidence	References
Stage I: Pre-155 Ma: East Gondwana affinity (Feature i)		
Triassic and Early Cretaceous dikes	Negative $\varepsilon_{Nd}(t)$ (-13.4 - -0.1) -$\varepsilon_{Hf}(t)$ (-24.2 - -0.1): a fragment of continental sliver	[1-3]
Late Triassic turbidite (NW Australia affinity)	NW, NE, E-W-directed paleocurrent (cross bedding)	[4, 5]
	peaks of 1250-900 and 750-450 Ma detrital zircons, and 400-200 Ma magmatic zircons with $\varepsilon_{Hf}(t)$ values of -10 - +14 correlate with those from the North Carnarvon Basin, NW Australia	[2, 6-8]
Late Jurassic conglomerate (Indian affinity)	NNE-directed paleocurrent (cross bedding)	[9]
	95% quartzite pebbles and detrital zircon peaks of 550 and 950 Ma	
Paleomagnetism	Triassic strata (Thakkhola): ca. 29.9°S, close to paleomagnetic reference frame of Indian APWP	[10]
Stage II: 155-152 Ma: Rifting of Argoland		
Longzi block and Tethys Himalaya: (Feature ii) Late Jurassic extension	**152.8 Ma alkaline magmatism in Mt. Kala**	**This study**
	147 Ma trachyandensitic (OIB-type) dike and 145 Ma diabase (MORB-type) dike	[11, 12]
	Thakkhola Graben and Nyalam: drastic changes in sedimentation from offshore to deltaic to shelf in Late Jurassic	[13]
NE Indian Ocean	152-155 Ma (Leg 261, Leg 765, CHRISP)	[14-16]
NW Australia	major unconformity (Callovian/Oxfordian); Rapid subsidence during the Tithonian (ca. 150 Ma)	[17]
	escarpment was rapidly and locally buried with 1200 m sediments by the end of the Callovian	[18]
Stage III: ca. 130 Ma: Subduction and collision		
Longzi block: post-rifting and pre-final collisional contractional deformation (Feature iii)	**Contractional deformation**: asymmetric folds in Triassic, Jurassic and Early Cretaceous strata, which are cut by Early Cretaceous dikes	**This study**
	Early Cretaceous dikes: 135-118 Ma	[3, 12, 19, 20]
	SSZ-affinity mafic dikes, andesite and silicic intrusions	[3, 21]
Neo-Tethys Ocean (an initiation of subduction)	SSZ-type ophiolites: 119-134 Ma	[22-25]
	Amphibolites: metamorphic sole: 123-135 Ma	[26-28]
	Zedang/Trans-Tethyan subduction system: 133-136 Ma, 152-163 Ma	[29-31]

References: (1) Huang et al., 2018; (2) Liu et al., 2020; (3) Wang et al., 2016b; (4) Li et al., 2003; (5) Zhang et al., 2019; (6) Cai et al., 2016; (7) Lewis & Sircombe, 2013; (8) Wang et al., 2016a; (9) Pan, 2018; (10) Klootwijk & Bingham, 1980; (11) Shi et al., 2018; (12) Zhu et al., 2008; (13) Garzanti, 1999; (14) Gibbons et al., 2012; (15) Heine & Muller, 2005; (16) Veevers et al., 1991; (17) Gradstein, 1992; (18) Veenstra, 1985; (19) Zhu et al., 2009; (20) Chen et al., 2018; (21) Ao et al., 2018; (22) Dai et al., 2013; (23) Hébert et al., 2012; (24) Zhang et al., 2016b; (25) Xiong et al., 2016; (26) Guilmette et al., 2009; (27) Guilmette et al., 2012; (28) Zhang et al., 2016a; (29) Buckman et al., 2018; (30) McDermid et al., 2002; (31) Zhang et al., 2014.

4.2 Late Jurassic rifting of the Longzi block

Geochemistry of mafic-ultramafic rocks in the Longzi block and their intrusive contacts with host clastic sediments (Figs. 6b-d, 7b) (also Liu et al., 2020) show they are Late Jurassic

alkali intrusions, rather than ophiolites representing suture zones within the Longzi block (Ao et al., 2018; Liu et al., 2020).

In the Himalaya, the thickness of Late Jurassic strata varies over short distances from a few tens to some hundred meters (Yin & Wan, 1996). They record a transition from offshore shales to local deltaic siliciclastics in the Tithonian-Berriasian; paleo-depth and environments progressively change from shelf to pelagic in the Valanginian-Albian, suggesting development of horst-and-graben structure related to the onset extensional tectonics (Garzanti, 1999; Yin & Wan, 1996).

The sedimentary succession and alkali magmatism collectively suggest that Late Jurassic rifting and extension is recorded in the rocks of the Longzi block (Figs. 8, 9b). These features fulfill the diagnostic feature ii mentioned in Introduction section (Table 1).

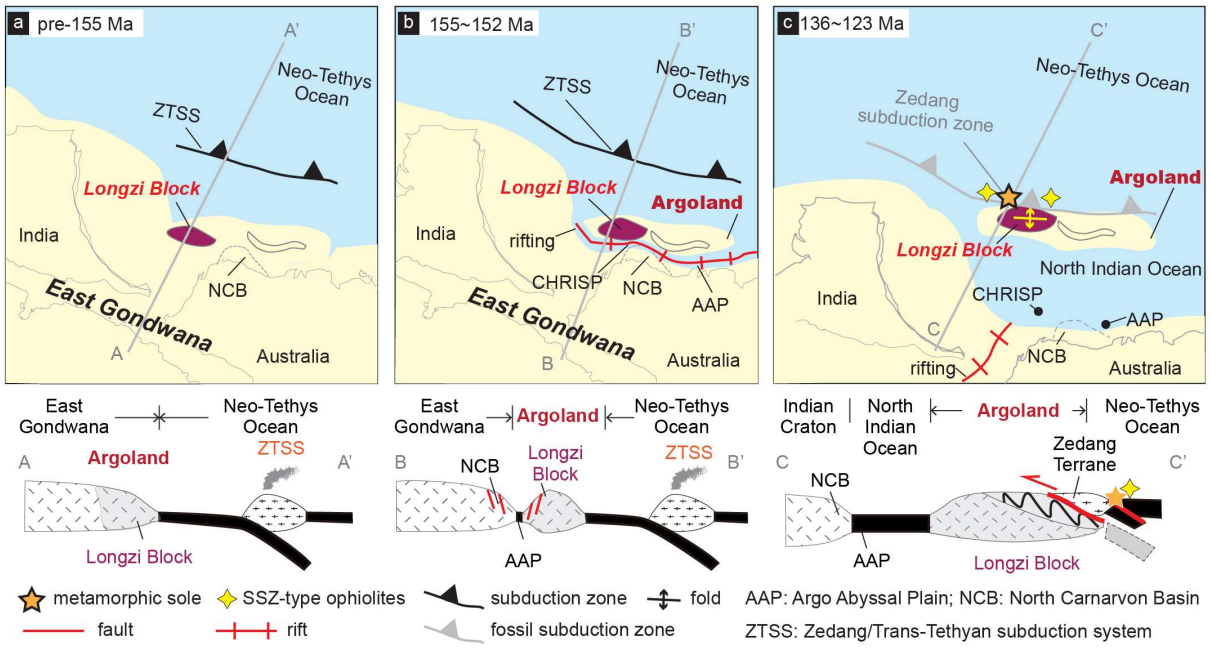

Figure 9. Reconstruction of paleogeography in Neo-Tethys Ocean and East Gondwana at (a) pre-155 Ma, and (b) Late Jurassic: the Longzi block attaches and rifts from the East Gondwana, respectively, and (c) Early Cretaceous: the Longzi block, the westernmost part of Argoland, drifts north from East Gondwana and collides with a north-dipping Trans-Tethyan subduction zone to generate the south-vergent folds in the Longzi block; the collision-triggered initial subduction in the Neo-Tethys Ocean generated metamorphic sole and SSZ-type ophiolites in the Yarlung belt at this time. We suppose that the Longzi block was longitudinally separated from the Indian continent, but they had similar paleo-latitude during Late Jurassic and Early Cretaceous time.

4.3 Longzi block as a fragment of Argoland from East Gondwana

4.3.1 Pre-155 Ma East Gondwana-affinity

Above relationships show that the Longzi block rifted from its host continent in Late Jurassic. The Mid-Late Triassic and Early Cretaceous dikes have negative $\varepsilon_{Nd}(t)$ (-13.4 - -0.1) and $\varepsilon_{Hf}(t)$ (-24.2 - -0.1) (Fig. 2a, Table 1), demonstrating that the Longzi block contains a basement of continental sliver, at odds with interpretation of this block as an accretionary complex (Ao et al., 2018).

Cross-bedding in Triassic strata record NW, NE and E-W directed paleocurrent (Figs. 2a, 8) (Li et al., 2003; Zhang et al., 2019). Detrital zircons with 1250-900 and 750-450 Ma, and 400-200 Ma magmatic age peaks and $\varepsilon_{Hf}(t)$ values of -10 - +14 correlate with those from the North Carnarvon Basin (Lewis & Sircombe, 2013), suggesting that the Triassic strata have NW Australia affinity (Table 1) (Cai et al., 2016; Liu et al., 2020; Wang et al., 2016a). The Late Jurassic conglomerates have NNE-directed paleocurrent (based on cross bedding) (Figs. 1b, 8) and Indian-derived 95% quartzite pebbles and detrital zircon peaks of 550 and 950 Ma (Pan, 2018). The above relationships show that the Longzi block in NE Himalaya was attached to East Gondwana before 155 Ma, which accords with paleomagnetic data in Triassic strata (Fig. 9a, Table 1) (Klootwijk & Bingham, 1980).

4.3.2 Late Jurassic breakup from East Gondwana as a westernmost Argoland

The Neo-Tethys Ocean suture zone is represented by the Yarlung belt and eastern Indo-Burma Range (Fig. 1b) (Aitchison et al., 2019). Middle Jurassic cherts from Indo-Burma Range ophiolitic mélanges (Aitchison et al., 2019; Zhang et al., 2018), and Late Anisian-Carnian chert and siltstone from Zedang City (Chen et al., 2019) and eastern Indo-Burma Range (Figs. 1b, 8) (Zhang et al., 2018) indicate Neotethyan spreading off of East Gondwana before the Middle-Late Triassic; the Longzi block was still attached East Gondwana at this time (Fig. 9a, Table 1).

Early Cretaceous contractional deformation suggests that the Longzi block had drifted away from its host East Gondwana which was a passive continental margin before that time (Fig. 8); Late Jurassic rapid changes of water depth of sedimentation (Yin & Wan, 1996) and alkali and MORB-type magmatism (Shi et al., 2018; Zhu et al., 2008 and this study) record extension and the rifting and drifting of the Longzi block between Late Jurassic and Early Cretaceous time (Figs. 8, 9b). Tithonian extension along northern margin of Indian plate (Figs. 1b, 8) (Garzanti, 1999; Yin & Wan, 1996) and 152-155 Ma NE Indian Ocean crust in the Argo Abyssal Plain and at CHRISP (Figs. 1a, 8) (Gibbons et al., 2012; Heine & Muller, 2005; Veevers et al., 1991; Zahirovic et al., 2016) are additional supporting evidence indicating that the Longzi block separated from East Gondwana in the Late Jurassic (Fig. 9b).

The extension and rifting was coeval with the development of an escarpment with 1200 m of sediments offshore of NW Australia that formed by faulting in Callovian to Upper Jurassic time (Table 1) (Gradstein, 1992; Veenstra, 1985). This faulting was associated with Late Jurassic break-up of the East Gondwana to generate Argoland fragments derived from northwest Australia that dispersed to various locations in SE Asia, such as Indo-Burma Range, West Sulawesi, SW Borneo, East Java and Woyla arc (Fig. 1a) (Advokaat et al., 2018; Metcalfe, 2011; Zahirovic et al., 2016). The geologic evidence summarized above fulfills the three diagnostic

features in the Introduction section and suggests that the Longzi block, separated from East Gondwana, was the westernmost Argoland (Fig. 9b).

Our model confirms the Longzi block of the NE Himalaya as a continental sliver. This demonstrates an archipelagic framework between the Indian and Eurasian plates since the Late Jurassic (Fig. 9b), and strengthens the similarity between inferred Neotethyan realm and its un-closed southeastern continuation in the SW Pacific region between SE Asia and Australia (Hall, 2012). It is in contrast to models proposing that the rifting and drifting of Tibetan Himalayan from Indian plate began at 118 Ma (van Hinsbergen et al., 2012, 2019; Yuan et al., 2020), or the break-up of Indian-Australian plates at ca. 130 Ma (Fig. 1c) (Harry et al., 2020; Zhu et al., 2007). Our model also contrasts with previous models that propose that a single Neo-Tethys Ocean, represented by Yarlung ophiolitic belt, separated the Indian-affinity Tibetan Himalaya from the Eurasian plate (e.g., Yin & Harrison, 2000; Zhu et al., 2013).

4.4 Early Cretaceous collision in the NE Himalaya and Effects on East Asia

In the Early Cretaceous, the Longzi block was located at 55.4º S, and remained at a latitude similar to the Indian plate until 118-75 Ma as suggested by paleomagnetic data (Fig. 9c) (van Hinsbergen et al., 2012, 2019; Yuan et al., 2020). The paleolatitude taken in concert with the geological evidence presented herein suggests that the Longzi block was longitudinally separated from the East Gondwana by the North Indian Ocean (Fig. 9c) (Yuan et al., 2020).

Early Cretaceous igneous rocks in the NE Himalaya with SSZ affinity (Wang et al., 2016b), such as some mafic dikes, the andesite and silicic intrusions (Ao et al., 2018) support a subduction-collision model. The asymmetric folds in the NE Himalaya have southward vergence suggesting they were formed by top-to-south shear (Figs. 2b, 3-5). These facts are better explained by collision of the Longzi block with a N-dipping intra-oceanic subduction zone located north of it (Fig. 9c), which would be the Trans-Tethyan subduction zone (Aitchison et al., 2000; Jagoutz et al., 2015) that began at least since 163-152 Ma at the Zedang area, and continued to 133-136 Ma (Figs. 8, 9) (Buckman et al., 2018; McDermid et al., 2002; Zhang et al., 2014).

Such an Early Cretaceous collision triggered an initiation of subduction north of the Trans-Tethyan intra-oceanic arc in the Neo-Tethys Ocean (Fig. 9c). The initial subduction generated the 135-123 Ma metamorphic sole in the Saga and Luobusa areas (Figs. 8, 9c) (Guilmette et al., 2009, 2012; Zhang et al., 2016a), and 119-134 Ma supra-subduction zone-type ophiolites along Yarlung ophiolitic belt (Dai et al., 2013; Hébert et al., 2012; Xiong et al., 2016; Zhang et al., 2016b).

The archipelagic configuration containing the Longzi continental sliver, the westernmost fragment of Argoland from ca. 155-152 Ma, and the Early Cretaceous collision between Longzi block and Trans-Tethyan subduction system explain the key features of previous models, and also extends our understanding of the Neotethyan architecture in SE Asia during Late Jurassic-Early Cretaceous.

This third continental sliver in NE Himalaya independently collided with Indian and Eurasian plates in Cenozoic, confirming the two-stage Cenozoic Indian-Eurasian collision (Gibbons et al., 2015; Jagoutz et al., 2015; van Hinsbergen et al., 2012, 2019; Yuan et al., 2020).

5 Conclusions

Based on our detailed field mapping, structural, geochemical and geochronological analyses, integrated with published data, we draw the following conclusions:

(1) The mafic-ultramafic rocks in Mt. Kala intrude Triassic strata, and contain 152.8 Ma gabbro and alkaline mafic dikes. Combined with angular unconformity in Thakkhola Graben and Nyalam, these relationships demonstrate Late Jurassic extension in NE Himalaya. This was coeval with the opening of the NE Indian Ocean and the rifting of the NW Australia, suggesting that the Longzi block in NE Himalaya rifted and drifted as a fragment of Argoland from East Gondwana at 155-152 Ma.

(2) In the NE Himalaya, buckle folds in Triassic, Jurassic and Early Cretaceous strata include asymmetric, overturned, isoclinal and open folds that have south vergence with E-W-trending hinges. These folds were cross-cut by 135-118 Ma dikes, recording Early Cretaceous contractional deformation in southern Tibet.

(3) The Longzi block collided with a Trans-Tethyan oceanic subduction system in the Early Cretaceous, long before final onset of the Indian-Eurasian collision, to generate the south-vergence contractional structures in NE Himalaya. This collisional event was approximately coeval with development of metamorphic soles beneath SSZ-type ophiolites to north of the Trans-Tethyan intra-oceanic arc along Yarlung suture zone.

Acknowledgments

We thank Douwe J. J. van Hinsbergen for constructive discussion on Argoland. Dr. Fulong Cai is thanked for discussion on the tectonic evolution of south Tibet. Dr. Zhenyu Chen and Shuaihua Song are thanked for field assistance. This work has been supported by the Strategic Priority Research Program (B) of CAS (XDB18030103), the NSFC (41888101) and the National Key R & D Program of China (2017YFC0601206).

References

Advokaat, E. L., M. L. M. Bongers, A. Rudyawan, M. K. BouDagher-Fadel, C. G. Langereis, and D. J. J. van Hinsbergen (2018), Early Cretaceous origin of the Woyla Arc (Sumatra, Indonesia) on the Australian plate, *Earth and Planetary Science Letters*, *498*, 348-361, doi:10.1016/j.epsl.2018.07.001

Aitchison, J. C., et al. (2019), Tectonic Evolution of the Western Margin of the Burma Microplate Based on New Fossil and Radiometric Age Constraints, *Tectonics*, *38*, 1718-1741, doi:10.1029/2018tc005049

Aitchison, J. C., Badengzhu, A. M. Davis, J. Liu, H. Luo, J. G. Malpas, I. R. C. McDermid, H. Wu, S. V. Ziabrev, and M.-f. Zhou (2000), Remnants of a Cretaceous intra-oceanic subduction system within the Yarlung–Zangbo suture (southern Tibet), *Earth and Planetary Science Letters*, *183*(1), 231-244, doi:10.1016/S0012-821X(00)00287-9

Ao, S., W. Xiao, B. F. Windley, J. E. Zhang, Z. Zhang, and L. Yang (2018), Components and structures of the eastern Tethyan Himalayan Sequence in SW China: Not a passive margin shelf but a mélange accretionary prism, *Geological Journal*, *53*, 2665-2689, doi:10.1002/gj.3103

Buckman, S., J. C. Aitchison, A. P. Nutman, V. C. Bennett, W. M. Saktura, J. M. J. Walsh, S. Kachovich, and H. Hidaka (2018), The Spongtang Massif in Ladakh, NW Himalaya: An Early Cretaceous record of spontaneous, intra-oceanic subduction initiation in the Neotethys, *Gondwana Research*, *63*, 226-249, doi:10.1016/j.gr.2018.07.003

BYGS (2004), Introduction on Geological map of Longzi County (1:250000: Bureau of Yunnan Geological Survey). pp270 (in Chinese)

Cai, F., L. Ding, A. K. Laskowski, P. Kapp, H. Wang, Q. Xu, and L. Zhang (2016), Late Triassic paleogeographic reconstruction along the Neo–Tethyan Ocean margins, southern Tibet, *Earth and Planetary Science Letters*, *435*, 105-114, doi:10.1016/j.epsl.2015.12.027

Chen, D. S., H. Luo, X. H. Wang, B. Xu, and A. Matsuoka (2019), Late Anisian radiolarian assemblages from the Yarlung-Tsangpo Suture Zone in the Jinlu area, Zedong, southern Tibet: Implications for the evolution of Neotethys, *Island Arc*, *28*(4), e12302, doi:10.1111/iar.12302

Chen, S. S., W. M. Fan, R. D. Shi, X. H. Liu, and X. J. Zhou (2018), 118–115 Ma magmatism in the Tethyan Himalaya igneous province: Constraints on Early Cretaceous rifting of the northern margin of Greater India, *Earth and Planetary Science Letters*, *491*, 21-33, doi:10.1016/j.epsl.2018.03.034

Dai, J. G., C. S. Wang, A. Polat, M. Santosh, Y. L. Li, and Y. K. Ge (2013), Rapid forearc spreading between 130 and 120Ma: Evidence from geochronology and geochemistry of the Xigaze ophiolite, southern Tibet, *Lithos*, *172-173*, 1-16, doi:10.1016/j.lithos.2013.03.011

Garzanti, E. (1999), Stratigraphy and sedimentary history of the Nepal Tethys Himalaya passive margin, *Journal of Asian Earth Sciences*, *17*(5), 805-827, doi:10.1016/S1367-9120(99)00017-6

Gibbons, A. D., U. Barckhausen, P. van den Bogaard, K. Hoernle, R. Werner, J. M. Whittaker, and R. D. Müller (2012), Constraining the Jurassic extent of Greater India: Tectonic evolution of the West Australian margin, *Geochemistry, Geophysics, Geosystems*, *13*(5), doi:10.1029/2011gc003919

Gibbons, A. D., S. Zahirovic, R. D. Müller, J. M. Whittaker, and V. Yatheesh (2015), A tectonic model reconciling evidence for the collisions between India, Eurasia and intra-oceanic arcs of the central-eastern Tethys, *Gondwana Research*, *28*(2), 451-492, doi:10.1016/j.gr.2015.01.001

Gradstein, F. M. (1992), Leg 122–123, northwestern Australian margin; A stratigraphic and paleogeographic summary, *Proceedings of Ocean Drilling Program, Scientific Results*, *123*, 801-816

Guilmette, C., R. Hébert, J. Dostal, A. Indares, T. Ullrich, É. Bédard, and C. Wang (2012), Discovery of a dismembered metamorphic sole in the Saga ophiolitic mélange, South Tibet: Assessing an Early Cretaceous disruption of the Neo-Tethyan supra-subduction zone and consequences on basin closing, *Gondwana Research*, *22*(2), 398-414, doi:10.1016/j.gr.2011.10.012

Guilmette, C., R. Hébert, C. Wang, and M. Villeneuve (2009), Geochemistry and geochronology of the metamorphic sole underlying the Xigaze Ophiolite, Yarlung Zangbo Suture Zone, South Tibet, *Lithos*, *112*(1), 149-162, doi:10.1016/j.lithos.2009.05.027

Hall, R. (2012), Late Jurassic-Cenozoic reconstructions of the Indonesian region and the Indian Ocean, *Tectonophysics*, *570*, 1-41

Harry, D. L., et al. (2020), Evolution of the Southwest Australian Rifted Continental Margin During Breakup of East Gondwana: Results From International Ocean Discovery Program Expedition 369, *Geochemistry, Geophysics, Geosystems*, *21*(12), e2020GC009144, doi:10.1029/2020GC009144

Hébert, R., R. Bezard, C. Guilmette, J. Dostal, C. S. Wang, and Z. F. Liu (2012), The Indus-Yarlung Zangbo ophiolites from Nanga Parbat to Namche Barwa syntaxes, southern Tibet: First synthesis of petrology, geochemistry, and geochronology with incidences on geodynamic reconstructions of Neo-Tethys, *Gondwana Research*, *22*(2), 377-397

Heine, C., and R. D. Muller (2005), Late Jurassic rifting along the Australian North West Shelf: margin geometry and spreading ridge configuration, *Australian Journal of Earth Sciences*, *52*(1), 27-39

Huang, Y., H. W. Cao, G. M. Li, S. M. Brueckner, Z. Zhang, L. Dong, Z. W. Dai, L. Lu, and Y. B. Li (2018), Middle–Late Triassic bimodal intrusive rocks from the Tethyan Himalaya in South Tibet: Geochronology, petrogenesis and tectonic implications, *Lithos*, *318-319*, 78-90, doi:10.1016/j.lithos.2018.08.002

Jagoutz, O., L. Royden, A. F. Holt, and T. W. Becker (2015), Anomalously fast convergence of India and Eurasia caused by double subduction, *Nature Geoscience*, *8*(6), 475-478, doi:10.1038/ngeo2418

Klootwijk, C. T., and D. K. Bingham (1980), The extent of greater India, III. Palaeomagnetic data from the Tibetan Sedimentary series, Thakkhola region, Nepal Himalaya, *Earth and Planetary Science Letters*, *51*(2), 381-405, doi:10.1016/0012-821X(80)90219-8

Lewis, C., and K. Sircombe (2013), Use of U-Pb geochronology to delineate provenance of North West Shelf Sediments, Australia, in *West Australian Basins Symposium (WABS) 2013*, edited by M. Keep and S. J. Moss, Perth Convention & Exhibition Centre, Perth WA, pp. 1-27

Li, X. H., Q. G. Zeng, and C. S. Wang (2003), Palaeocurrent data: evidence for the source of the Langjiexue Group in southern Tibet, *Geological Review*, *49*(2), 132-137 (in Chinese with English abstract)

Liu, Y. M., J. G. Dai, C. S. Wang, H. A. Li, Q. Wang, and L. L. Zhang (2020), Provenance and tectonic setting of Upper Triassic turbidites in the eastern Tethyan Himalaya: Implications for early-stage evolution of the Neo–Tethys, *Earth-Science Reviews*, *200*, 103030, doi:10.1016/j.earscirev.2019.103030

McDermid, I. R. C., J. C. Aitchison, A. M. Davis, T. M. Harrison, and M. Grove (2002), The Zedong terrane: a Late Jurassic intra-oceanic magmatic arc within the Yarlung–Tsangpo suture zone, southeastern Tibet, *Chemical Geology*, *187*, 267-277

Metcalfe, I. (2011), Tectonic framework and Phanerozoic evolution of Sundaland, *Gondwana Research*, *19*, 3-21

Pan, W. Y. (2018), The sedimentary features and paleogeographic implication of the Late Jurassic quartz sandstones in Tethys Himalaya of southern Tibet. Master degree. China University of Geosciences (Beijing). 1-66 (in Chinese with English abstract) pp

Searle, M. P., and P. J. Treloar (2019), Introduction to Himalayan tectonics: a modern synthesis, *Geological Society, London, Special Publications*, *483*(1), 1-17, doi:10.1144/sp483-2019-20

Shi, Y. R., C. Y. Hou, J. L. Anderson, T. S. Yang, Y. M. Ma, W. W. Bian, and J. J. Jin (2018), Zircon SHRIMP U–Pb age of Late Jurassic OIB-type volcanic rocks from the Tethyan Himalaya: constraints on the initial activity time of the Kerguelen mantle plume, *Acta Geochimica*, *37*(3), 441-455, doi:10.1007/s11631-017-0239-2

Sun, S. S., and W. F. McDonough (1989), Chemical and isotopic systematic of oceanic basalt: implication for mantle composition and processes, in *Magmatism in the Oceanic Basins. Geological Society of London, Special publications 42*, edited by A. D. Saunders and M. J. Norry, pp. 313-346

van Hinsbergen, D. J. J., P. C. Lippert, G. Dupont-Nivet, N. McQuarrie, P. V. Doubrovine, W. Spakman, and T. H. Torsvik (2012), Greater India Basin hypothesis and a two-stage Cenozoic collision between India and Asia, *Proceedings of the National Academy of Sciences*, *109*(20), 7659-7664, doi:10.1073/pnas.1117262109

van Hinsbergen, D. J. J., P. C. Lippert, S. Li, W. Huang, E. L. Advokaat, and W. Spakman (2019), Reconstructing Greater India: Paleogeographic, kinematic, and geodynamic perspectives, *Tectonophysics*, *760*, 69-94, doi:10.1016/j.tecto.2018.04.006

Veenstra, E. (1985), Rift and drift in the Dampier sub-basin, a seismic and structural interpretation, *The APPEA Journal*, *25*(1), 177-189, doi:10.1071/AJ84016

Veevers, J. J., C. M. Powell, and S. R. Roots (1991), Review of seafloor spreading around Australia. I. Synthesis of the patterns of spreading, *Australian Journal of Earth Sciences*, *38*(4), 373-389

Wang, J. G., F. Y. Wu, E. Garzanti, X. M. Hu, W. Q. Ji, Z. C. Liu, and X. C. Liu (2016a), Upper Triassic turbidites of the northern Tethyan Himalaya (Langjiexue Group): The terminal of a sediment-routing system sourced in the Gondwanide Orogen, *Gondwana Research*, *34*, 84-98, doi:10.1016/j.gr.2016.03.005

Wang, Y. Y., L. E. Guo, L. S. Zeng, F. K. Chen, K. J. Hou, Q. Wang, L. H. Zhao, and J. H. Guo (2016b), Multiple phases of cretaceous magic magmatism in the Gyangze-Kangma area (Tethyan Himalaya) southern Tibet, *Acta Petrologica Sinica*, *32*(12), 3572-3596 (in Chinese with English abstract)

Winchester, J. A., and P. A. Floyd (1977), Geochemical discrimination of different magma series and their differentiation products using immobile elements, *Chemical Geology*, *20*, 325-343

Xiong, Q., W. L. Griffin, J.-P. Zheng, S. Y. O'Reilly, N. J. Pearson, B. Xu, and E. A. Belousova (2016), Southward trench migration at ~130–120 Ma caused accretion of the Neo-Tethyan forearc lithosphere in Tibetan ophiolites, *Earth and Planetary Science Letters*, *438*, 57-65, doi:10.1016/j.epsl.2016.01.014

Yao, W., L. Ding, F. L. Cai, H. Q. Wang, Q. Xu, and T. Zaw (2017), Origin and tectonic evolution of upper Triassic Turbidites in the Indo-Burma Ranges, West Myanmar, *Tectonophysics*, *721*, 90-105

Yin, A., and T. M. Harrison (2000), Geologic evolution of the Himalayan-Tibetan orogen, *Annual Reviews of Earth and Planetary Sciences*, *28*, 211-280

Yin, J. R., and X. Q. Wan (1996), Jurassic ammonite morphotypes as water-depth indicator of Tethys-Himalaya sea, *Acta Palaeontologica Sinica*, *35*(6), 734-751 (in Chinese with English

abstract)

Yuan, J., et al. (2020), Rapid drift of the Tethyan Himalaya terrane before two-stage India-Asia collision, *National Science Review*, doi:10.1093/nsr/nwaa173

Zahirovic, S., K. J. Matthews, N. Flament, R. D. Müller, K. C. Hill, M. Seton, and M. Gurnis (2016), Tectonic evolution and deep mantle structure of the eastern Tethys since the latest Jurassic, *Earth-Science Reviews*, *162*, 293-337, doi:10.1016/j.earscirev.2016.09.005

Zhang, B. S., Y. S. Wei, E. Garzanti, C. S. Wang, X. Chen, W. Y. Pan, and Q. S. Liu (2019), Sedimentologic and stratigraphic constraints on the orientation of the Late Triassic northern Indian passive continental margin, *Palaeogeography, Palaeoclimatology, Palaeoecology*, *533*, 109234, doi:10.1016/j.palaeo.2019.109234

Zhang, C., C. Z. Liu, F. Y. Wu, L. L. Zhang, and W. Q. Ji (2016a), Geochemistry and geochronology of mafic rocks from the Luobusa ophiolite, South Tibet, *Lithos*, *245*, 93-108, doi:10.1016/j.lithos.2015.06.031

Zhang, J. E., W. Xiao, B. F. Windley, J. Wakabayashi, F. Cai, K. Sein, H. Wu, and S. Naing (2018), Multiple alternating forearc- and backarc-ward migration of magmatism in the Indo-Myanmar Orogenic Belt since the Jurassic: Documentation of the orogenic architecture of eastern Neotethys in SE Asia, *Earth-Science Reviews*, *185*, 704-731, doi:10.1016/j.earscirev.2018.07.009

Zhang, L. L., C. Z. Liu, F. Y. Wu, W. Q. Ji, and J. G. Wang (2014), Zedong terrane revisited: An intra-oceanic arc within Neo-Tethys or a part of the Asian active continental margin?, *Journal of Asian Earth Sciences*, *80*, 34-55, doi:10.1016/j.jseaes.2013.10.029

Zhang, L. L., C. Z. Liu, F. Y. Wu, C. Zhang, W. Q. Ji, and J. G. Wang (2016b), Sr–Nd–Hf isotopes of the intrusive rocks in the Cretaceous Xigaze ophiolite, southern Tibet: Constraints on its formation setting, *Lithos*, *258-259*, 133-148, doi:10.1016/j.lithos.2016.04.026

Zhu, D. C., X. X. Mo, G. T. Pan, Z. D. Zhao, G. C. Dong, Y. R. Shi, Z. L. Liao, L. Q. Wang, and C. Y. Zhou (2008), Petrogenesis of the earliest Early Cretaceous mafic rocks from the Cona area of the eastern Tethyan Himalaya in south Tibet: Interaction between the incubating Kerguelen plume and the eastern Greater India lithosphere?, *Lithos*, *100*(1), 147-173, doi:10.1016/j.lithos.2007.06.024

Zhu, D. C., G. T. Pan, X. X. Mo, Z. L. Liao, X. S. Jiang, L. Q. Wang, and Z. D. Zhao (2007), Petrogenesis of volcanic rocks in the Sangxiu Formation, central segment of Tethyan Himalaya: A probable example of plume–lithosphere interaction, *Journal of Asian Earth Sciences*, *29*(2), 320-335, doi:10.1016/j.jseaes.2005.12.004

Zhu, D. C., Y. Xia, B. B. Qiu, Q. Wang, and Z. D. Zhao (2013), Why do we need to propose the Early Cretaceous Comei large igneous province in southeastern Tibet?, *Acta Petrologica Sinica*, *29*(11), 3659-3670 (in Chinese with English abstract)